Mixed-Halide MX Chain Solids: Effect of Chloride Doping on the Crystal Structure and Resonance Raman Spectra of $[Pt(en)_2Br_2][Pt(en)_2](ClO_4)_4$

Sara C. Huckett,† Robert J. Donohoe,† Laura A. Worl,† Alain D. F. Bulou,† Carol J. Burns,† Joseph R. Laia,‡ David Carroll,‡ and Basil I. Swanson*,†

Inorganic and Structural Chemistry Group (INC-4) and Materials Technology: Polymers & Coatings Group (MST-7), Los Alamos National Laboratory, Los Alamos, New Mexico 87545

Received May 30, 1990. Revised Manuscript Received October 10, 1990

The crystal structure and resonance Raman spectra of $[Pt(en)_2][Pt(en)_2Br_2](ClO_4)_4$ (PtBr, where en = $H_2NCH_2CH_2NH_2$) have been studied as a function of chloride ion doping and temperature. Chloride ion doping in PtBr results in crystalline solids with a solid solubility that ranges from pure PtBr to pure PtCl. These results show that the previously reported monoclinic and orthorhombic forms of PtBr arise from differing chloride impurity concentrations and resulting changes in critical temperature (T_c); PtBr, PtCl, and mixed PtBr/PtCl solids are demonstrated to undergo phase transformations with increasing temperatures (T_c = 19.8 °C (PtCl), 25.5 °C ($PtBr_{0.45}Cl_{0.55}$), 28.7 °C ($PtBr_{0.99}Cl_{0.01}$)). Resonance Raman fine structure for the the chain axis ν_1 mode, along with several other resonance-enhanced defect vibrations, are shown to result from chloride ion impurities in the PtBr solid.

Introduction

$[Pt(en)_2][Pt(en)_2Br_2](ClO_4)_4$ (PtBr, where en = $H_2NCH_2CH_2NH_2$) is an example of a halide-bridged mixed-valence metal complex (MX solid) composed of alternating Pt(II) and Pt(IV) centers linearly bridged by bromide ions. Early interest in MX solids was stimulated by their anisotropic optical, electronic, and vibrational properties.[1] MX solids are strongly correlated, low-dimensional electronic materials for which the electron-electron and electron-phonon forces can be chemically tuned so as to drive them from a Peierls distorted charge density wave (CDW) to a spin density wave (SDW) ground state.[2] Earlier X-ray diffraction and resonance Raman (RR) studies of PtBr have shown surprisingly complex structural and spectral behavior.

Resonance Raman (RR) spectroscopy has proven to be a useful probe of the ground-state and defect (polarons, bipolarons, kinks, and excitons) properties of MX solids.[3] Clark and Kurmoo[4] reported the first study of dispersion of the Raman-active ν_1 mode with respect to excitation energy for the CDW solids PtX (X = Cl, Br, I). As the excitation energy increased (from 1.83 to 2.71 eV), they observed a monotonic wavenumber shift for ν_1. Upon noting that the magnitude of the ν_1 shift depended on the halide (3, 14, and 16 cm^{-1} for PtCl, PtBr, and PtI, respectively), Clark and Kurmoo suggested that this dispersion is controlled by the extent of valence delocalization along the chain and, therefore, is related to the one-dimensional semiconducting nature of the chain.

Subsequent RR studies of oriented single crystals of PtBr at low temperatures (4-15 K)[3a,c] have demonstrated that the dispersion results from fine structure of the ν_1 band that consists of components whose relative intensities depend on the excitation energy. By analogy to the *trans*-polyacetylene system,[5] the origin of this fine structure was attributed by Tanaka and Kurita to the presence of chains of different correlation lengths. On the basis of the sample dependence of the relative intensities of the ν_1 components, Conradson et al. attributed the fine structure to the presence of structurally distinct species that arise due to local interchain ordering and/or defects.[3c]

Crystallographic measurements are crucial for understanding the electronic and lattice dynamics properties of MX materials. However, ambiguous behavior has been observed in the crystallography of PtBr; four different crystal structures have been reported.[6] These structures of PtBr have proven to be sample dependent and surprisingly different from those of PtCl and PtI. Both monoclinic and orthorhombic forms have been reported for crystals grown at ambient pressure,[6a,b] and at 7 kbar PtBr crystallizes in a monoclinic cell with a slightly different chain packing arrangement.[6c] Keller et al. reported that PtBr undergoes a monoclinic to orthorhombic structural phase transformation under Cu Kα irradiation.[6a]

We show here that the fine structure of the PtBr ν_1 vibration observed upon tuning the excitation energy through the IVCT band results, in large measure, from chloride impurities that are generated during the preparation of PtBr by using the normal synthetic route. We also show that the different crystalline modifications of PtBr, the monoclinic and orthorhombic forms, arise from differing chloride impurity levels and that pure PtBr and PtCl undergo structural phase transformations with temperature. The nature of the defects/microstructures that give rise to the ν_1 components, as well as other Raman

† Inorganic and Structural Chemistry Group.
‡ Materials and Technology: Polymers & Coatings Group.

(1) See, for example: Miller, J. S.; Epstein, A. J. *Prog. Inorg. Chem.* **1976**, *20*, 1 and references therein.
(2) (a) Toriumi, K.; Wada, Y.; Mitani, T.; Bandow, S. *J. Am. Chem. Soc.* **1989**, *111*, 2341. (b) Gammel, J. T.; Batistic, I.; Bishop, A. R.; Loh, E. Y., Jr.; Marianer, S. In *Proceedings of the International Conference on Highly Correlated Electron Systems, 1989*; Santa Fe, NM, in press.
(3) (a) Tanaka, M.; Kurita, S. *J. Phys. C* **1986**, *19*, 3019. (b) Clark, R. J. H.; Croud, V. B. In *Organic and Inorganic Low-Dimensional Crystalline Materials*; Delhaes, P., Drillon, M., Eds.; Plenum: New York, 1987. (c) Conradson, S. D.; Dallinger, R. F.; Swanson, B. I.; Clark, R. J. H.; Croud, V. B. *Chem. Phys. Lett.* **1987**, *135*, 463. (d) Donohoe, R. J.; Ekberg, S. A.; Tait, C. D.; Swanson, B. I. *Solid State Commun.* **1989**, *71*, 49. (e) Fanizzi, F. P.; Natile, G.; Tiripicchio, A.; Clark, R. J. H.; Michael, D. J. *J. Chem. Soc., Dalton Trans.* **1989**, 1689. (f) Donohoe, R. J.; Dyer, R. B.; Swanson, B. I. *Solid State Commun.* **1990**, *73*, 521. (g) Donohoe, R. J.; Tait, C. D.; Swanson, B. I. *Chem. Mater.* **1990**, *2*, 315.
(4) Clark, R. J. H.; Kurmoo, M. *J. Chem. Soc., Faraday Trans.* **1983**, *79*, 519.
(5) (a) Kuzmany, H. *Phys. Status Solidi* **1980**, *b97*, 521. (b) Kuzmany, H.; Imhoff, E. A.; Fitchen, D. B.; Sarhangi, A. *Phys. Rev. B* **1982**, *26*, 7109.
(6) (a) Keller, H. J.; Muller, B.; Ledezma, G.; Martin, R. *Acta Crystallogr.* **1985**, *C41*, 16. (b) Endres, H.; Keller, H. J.; Martin, R.; Traeger, U.; Novotny, M. *Acta Crystallogr.* **1980**, *B36*, 35. (c) Weinrach, J. B.; Ekberg, S. A.; Conradson, S. D.; Swanson, B. I.; Hochheimer, H. D. *Inorg. Chem.* **1990**, *29*, 981.

0897-4756/91/2803-0123$02.50/0

Table I. Cell Constants for Pure and Mixed PtBr and PtCl Crystals[a]

compd	cryst system/space group	a	b	c	β	V
PtCl[b]	orthorhombic	9.643 (1)	10.807 (2)	13.525 (2)		1409.4
$PtBr_{0.22}Cl_{0.78}$	orthorhombic	9.660 (2)	10.841 (2)	13.546 (3)		1418.5 (6)
$PtBr_{0.45}Cl_{0.55}$	monoclinic	7.908 (11)	10.877 (6)[c]	8.525 (10)	109.17 (10)	692.6 (7)
		9.536[d]	10.877	13.397	85.45	1385.2
$PtBr_{0.98}Cl_{0.02}$	monoclinic	7.959 (1)	10.962 (3)	8.529 (2)	109.33 (2)	702.1 (48)
		9.547[d]	10.962	13.455	85.80	1404.3
$PtBr_{0.98}Cl_{0.02}$[e]	orthorhombic	9.655	10.963[c]	13.596		1439.2

[a] All measurements were made at room temperature unless otherwise noted; all lengths, angles, and volumes are given in Å, deg, and Å^3, respectively. [b] Reference 13. The axis assignments have been changed from those reported. [c] No k odd reflections were observed in the reflections used for indexing; therefore, this axis was doubled by matrix multiplication. [d] The monoclinic cell has been transformed to a pseudoorthorhombic cell. [e] Data were obtained at ~40 °C.

active modes observed with excitation above and below the IVCT band edge, will be discussed in more detail elsewhere.

Experimental Section

PtBr was synthesized by three methods. In method A, $Pt(en)_2Cl_2$ was oxidized with Br_2, the excess Br_2 removed, and the resulting solution of $[Pt(en)_2Br_2]Cl_2$ reacted with $Pt(en)_2Cl_2$.[7] The product was precipitated by dropwise addition of 60% $HClO_4$ and recrystallized from water by slow evaporation at ~34 °C to produce dark green crystals. In a typical preparation, $[Pt(en)_2Br_2]Cl_2$ (1.04 mmol) in 10 mL of deionized H_2O was combined with $Pt(en)_2Cl_2$ (1.04 mmol) in 10 mL of H_2O, and PtBr was precipitated from the solution with 2 mL of 60% $HClO_4$. These crystals were filtered, dissolved in ~45 mL of H_2O, and the solution was refiltered. Slow evaporation of this solution at ~34 °C produced several crystals (approximate dimensions 0.5 cm × 0.2 cm × 0.1 cm) after 11 days. In method B, $Pt(en)_2(ClO_4)_2$ was produced by reaction of excess $AgClO_4$ with $Pt(en)_2Cl_2$. The $Pt(en)_2(ClO_4)_2$ was precipitated by addition of EtOH, filtered, washed, and then immediately redissolved in deionized H_2O. Half the $Pt(en)_2(ClO_4)_2$ was oxidized with Br_2 and reacted with the remaining $Pt(en)_2(ClO_4)_2$, and the product precipitated and recrystallized as for A to give bright green crystals. In method C, $Pt(en)_2Br_2$ was synthesized by treatment of $Pt(en)_2(ClO_4)_2$ with HBr.[8] The product was then obtained via method A with $Pt(en)_2Br_2$ substituted for $Pt(en)_2Cl_2$. The $PtBr_{0.05}Cl_{0.95}$ sample was prepared by slow evaporation of a solution containing 92 and 8 mol % of PtCl and $PtBr_{0.99}Cl_{0.01}$, respectively.

^{1}H NMR spectra of crystals dissolved in D_2O were obtained on a Bruker WM-300 spectrometer and referenced to the internal H_2O impurity (4.63 ppm). $PtBr_{1-x}Cl_x$ compositions are reported as mole percentages of the total halide content and determined by integration of ^{1}H NMR spectra. Error inherent in the integration procedure (~5%) is compounded by the error in integrating unresolved peaks and adding/subtracting contributions from the Pt satellites. The reliability of this method is demonstrated by elemental analysis (Galbraith Laboratories, Inc.) of pieces of crystals whose composition had been determined by ^{1}H NMR: (a) $PtBr_{0.88}Cl_{0.12}$ 7.86% C, 2.80% H, and 11.69% Br (calcd 8.16% C, 2.72% H, and 11.94% Br for $PtBr_{0.88}Cl_{0.12}$); (b) $PtBr_{0.97}Cl_{0.03}$ 7.96% C, 2.75% H, 13.68% Br, and 12.38% Cl (calcd 8.09% C, 2.72% H, 13.45% Br, and 11.93% Cl for pure PtBr). Where PtCl percentages are reported, both NMR and either X-ray, RR, or differential scanning calorimetry (DSC) measurements were made using pieces of the same crystal. Exceptions are (a) $PtBr_{0.98}Cl_{0.02}$, Table I (a large $PtBr_{0.98}Cl_{0.02}$ crystal was dissolved and no further NMR measurements made after recrystallization at 0 °C) and (b) $PtBr_{0.22}Cl_{0.78}$, Table I and Figure 3c (the Cl^- content was estimated from a linear plot of percent Cl and b-axis length). Raman spectra were obtained from single-crystal samples at 12 K with incident intensities less than 2 mW. Laser excitation was provided by a Spectra Physics Model 3900 Ti:sapphire solid state laser pumped by a Spectra Physics Model 2040 Ar^+ laser. The scattered light was coupled into a SPEX 1877D triple spectrograph equipped with a liquid nitrogen cooled Photometrics PM512 grade prime CCD. Differential scanning calorimetry was performed under Ar by using an omnitherm OSG-1200 with a high-temperature head at a ramp rate of 2 °C/min. The system was calibrated with respect to temperature and enthalpy by using the phase transformations of In and Ga at 156.3 and 29.78 °C, respectively.

X-ray diffraction was performed on either an Enraf-Nonius CAD-4 or a Siemens R3MN automated diffractometer using Mo $K\alpha$ radiation (λ = 0.71069 Å) run by a MicroVax 11 local network. All cell constants and volumes are given in Å and Å^3, respectively. Crystals used for diffraction were produced by slow evaporation at ~34 °C with the exception of $PtBr_{0.98}Cl_{0.02}$, which was crystallized from H_2O at 0 °C.

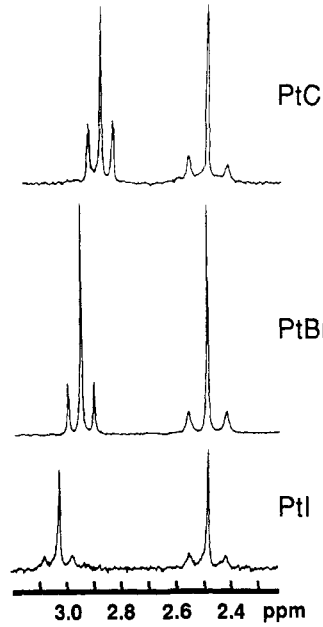

Figure 1. ^{1}H NMR spectra of PtX complexes (D_2O).

Results and Discussion

Synthesis of PtBr has traditionally proceeded via method A[7] as described in the Experimental Section. However, this method leads to chloride impurities in the crystalline PtBr product that have been identified by ^{1}H NMR after redissolution. The NMR measurement of redissolved PtBr has proven useful for detection of small amounts (<5%) of PtCl impurities that are difficult to detect when using other techniques such as elemental analysis. ^{1}H NMR spectra of PtX (Figure 1) show the methylene proton resonances for the $Pt(en)_2^{2+}$ and $Pt(en)_2X_2^{2+}$ subunits: these occur at δ 2.51 (triplet (t), J_{Pt-H} = 20.3 ± 0.2 Hz) and at 2.87 (X = Cl, t, J_{Pt-H} = 12.5 ± 0.3 Hz), 2.94 (X = Br, t, J_{Pt-H} = 13.3 ± 0.2 Hz), and 3.03 (X = I, t, J_{Pt-H} = 15.7 ± 0.2 Hz). Spectra of PtBr contaminated with >5–10% PtCl also show a resonance corresponding to $Pt(en)_2ClBr^{2+}$ at 2.91 ppm (at lower percentages of PtCl, this signal is obscured by the PtBr

(7) Bekaroglu, O.; Breer, H.; Endres, H.; Keller, H. J.; Nam Gung, H. *Inorg. Chem. Acta* **1977**, *21*, 183.
(8) Hantzsch, H.; Rosenblatt, F. *Z. Anorg. Allg. Chem.* **1930**, *187*, 241.

platinum satellite). Observation of $Pt(en)_2ClBr^{2+}$ in the solution spectra does not necessarily demonstrate the presence of $Pt(en)_2ClBr^{2+}$ units in the solid material; mixing of pure solutions of $Pt(en)_2Br_2^{2+}$ and $Pt(en)_2Cl_2^{2+}$ in the presence of $Pt(en)_2^{2+}$ leads to rapid (<20 min) formation of the same peak. However, this result clearly refutes the conclusion[9] that $Pt(en)_2ClBr^{2+}$ units are forbidden in mixed PtCl/PtBr crystals due to the stability of $Pt(en)_2X_2^{2+}$ species in solution.

The presence of chloride ion in the product can be attributed to two factors. The first is Pt(II) catalysis of Pt(IV) substitution reactions.[10] The exchange of Cl^- in $Pt(en)_2Cl_2^{2+}$ with Br^- has been reported,[11] and at an ionic strength of 0.5 M (20 °C) the equilibrium constants were found to be

$$K_1 = [Pt(en)_2ClBr^{2+}][Cl^-]/[Pt(en)_2Cl_2^{2+}][Br^-] = 11.5$$

$$K_2 = [Pt(en)_2Br_2^{2+}][Cl^-]/[Pt(en)_2ClBr^{2+}][Br^-] = 4.3$$

These values clearly illustrate the feasibility of producing either $Pt(en)_2ClBr^{2+}$ or $Pt(en)_2Cl_2^{2+}$ in the reaction mixture (method A), where the overall concentration of Br^-:Cl^- is 1:2, and result in the formation of ~11% PtCl in the PtBr product. The second contributing factor is an en·2HCl impurity in the $Pt(en)_2Cl_2$ starting material. This impurity (^1H NMR, D_2O, δ = 3.19) is generated by reaction of en and HCl and, because it has solubility properties similar to those of $Pt(en)_2Cl_2$, can be difficult to remove by recrystallization. Due to the substitution reactions of $Pt(en)_2Br_2^{2+}$ and Cl^-, the net effect of the en·2HCl impurity is to increase the amount of PtCl doping of PtBr. This was illustrated by employing $Pt(en)_2Cl_2$ contaminated with an approximately equimolar amounts of en·2HCl in the synthesis of PtBr via method A. A large crystal, $PtBr_{0.45}Cl_{0.55}$, was initially harvested from the solution, and crystals obtained by further evaporation of the solution were shown, by RR, to contain an even higher percentage of PtCl. When $Pt(en)_2Cl_2$ free from the en·2HCl is used, $PtBr_{0.89}Cl_{0.11}$ is obtained.

In attempts to prepare pure PtBr, methods B and C were employed and produced $PtBr_{0.97}Cl_{0.03}$ and $PtBr_{0.99}Cl_{0.01}$, respectively. The amounts of PtCl impurities can vary slightly from preparation to preparation; method B was subsequently used to give $PtBr_{0.98}Cl_{0.02}$. The source of Cl^- in these preparative routes is not obvious but could arise from incomplete Cl^- abstraction due to the presence of very low concentrations of dimeric platinum species in solution.

The $PtBr_{0.99}Cl_{0.01}$ crystals as well as the pure PtCl material have been structurally characterized by temperature-dependent X-ray diffraction[12] and by differential scanning calorimetry (Figure 2). The cell constants for these systems are given in Table I; in all cases, the *b* parameter corresponds to the chain axis. These data illustrate two basic effects of doping on the PtBr crystal structure. The first is contraction of the chain axis on going from $PtBr_{0.98}Cl_{0.02}$ to $PtBr_{0.45}Cl_{0.55}$, $PtBr_{0.22}Cl_{0.78}$, and finally pure PtCl.[13] On the basis of the available data and as expected for a one-dimensional chain, this contraction along the chain axis is linear with respect to an increase in the concentration of the smaller Cl^- ions.

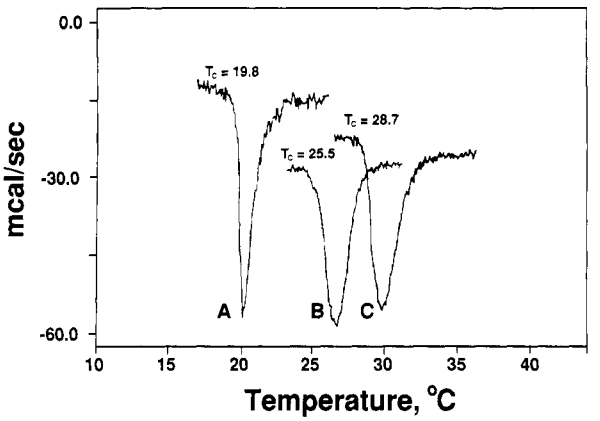

Figure 2. Differential scanning calorimetry endotherms for (A) pure PtCl, (B) $PtBr_{0.45}Cl_{0.55}$, and (C) $PtBr_{0.99}Cl_{0.01}$.

The second effect of Cl^- doping on the PtBr structure is a change in the crystal system. PtBr has usually been found to crystallize in a monoclinic phase,[6a,c,7] although orthorhombic PtBr has also been reported.[6a,b] In contrast, only orthorhombic PtCl has been reported.[13] DSC of $PtBr_{0.99}Cl_{0.01}$ shows that a phase change occurs between 27 and 32 °C (the onset is observed at 28.7 ± 0.2 °C with an enthalpy of 3.08 ± 0.05 kcal/mol; see Figure 2). The phase change observed by X-ray crystallography revealed a monoclinic to orthorhombic structural rearrangement; cell constants for a monoclinic $PtBr_{0.98}Cl_{0.02}$ crystal were obtained at room temperature (Table I), and then the crystal heated to ~40 °C on the diffractometer. From 25 reflections, cell constants corresponding to an orthorhombic cell (Table I) were then calculated. For $PtBr_{0.22}Cl_{0.78}$ and for pure PtCl only the orthorhombic form is observed at room temperature.

The critical temperature (T_c) for the observed phase change for mixed crystals depends on and provides a measure of the Cl^- impurity level. DSC measurements for pure PtCl show that it undergoes a phase change (the onset temperature is observed at 19.8 ± 0.2 °C with an enthalpy of 2.66 ± 0.09 kcal/mol) similar to that observed for the $PtBr_{0.99}Cl_{0.01}$. Both PtCl and $PtBr_{0.99}Cl_{0.01}$ show slight hysteresis (2.2 ± 0.2 and 2.6 ± 0.2 °C, respectively) as is consistent with first-order phase transformations. In both materials the lower temperature monoclonic phase was found to be $P2_1/m$ and the high-temperature space group *lbam*.[12] The endotherms observed for PtCl, $PtBr_{0.99}Cl_{0.01}$, and $PtBr_{0.45}Cl_{0.55}$ are compared in Figure 2. Note that the critical temperature for the $PtBr_{0.45}Cl_{0.55}$ sample is between those for the pure PtCl and $PtBr_{0.99}Cl_{0.01}$ samples and that the endotherm has essentially the same shape as that for $PtBr_{0.99}Cl_{0.01}$. On the basis of the above DSC data and the observation of good single-crystal diffraction data for mixed Br/Cl samples, we conclude that Cl^- ion doping of PtBr results in homogenous crystalline materials.

The above results provide an explanation for the monoclinic to orthorhombic phase change observed earlier under Cu Kα irradiation.[6a] The 10.914-Å *b* axis measured in this earlier study indicates a significant amount of Cl^- impurity (~32% by comparison to a linear plot of *b*-axis length vs percent Cl). On the bais of DSC data (Figure 2), which shows $PtBr_{0.45}Cl_{0.55}$ to have T_c = 25.54 °C, the transition to the orthorhombic phase is expected to occur at ~26 °C and could result from heating in the X-ray beam. The structural phase transformation involves an increase in the *a* and *c* axes, a commensurate increase in the cell volume, and a surprisingly large change in the pseudoorthorhombic β angle (compare in Table I, $PtBr_{0.98}Cl_{0.02}$ pseudoorthorhombic cell at room temperature

(9) Tanino, H.; Takahashi, K.; Kato, M.; Yao, T. *Solid State Commun.* **1988**, *65*, 643.
(10) Hartley, F. R. *The Chemistry of Platinum and Palladium*; Applied Science: London, 1973.
(11) Poe, A. J. *J. Chem. Soc.* **1963**, 183.
(12) Huckett, S. C.; Garcia, E.; Swanson, B. I., manuscript in preparation.
(13) Matsumoto, N.; Yamashita, M.; Ueda, I.; Kida, S. *Memoirs of the Faculty of Science; Kyushu University Series C* **1978**, *11*, 209.

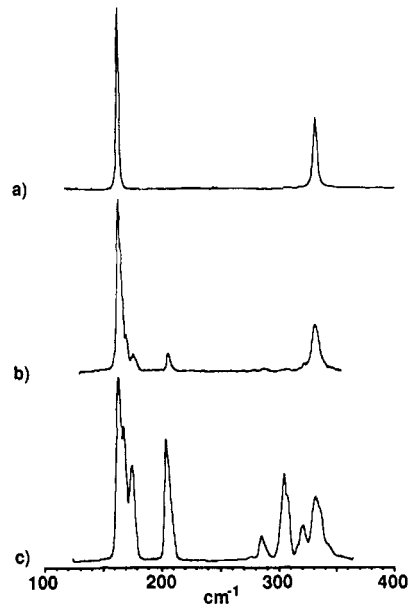

Figure 3. Resonance Raman spectra of (a) $PtBr_{0.99}Cl_{0.01}$, (b) $PtBr_{0.89}Cl_{0.11}$, and (c) $PtBr_{0.22}Cl_{0.78}$ at 1.60-eV excitation.

and the high-temperature orthorhombic cell). The phase change does not affect the metal–halide linear chain (*b*) axis and involves a rearrangement of the ClO_4^- counterions and a rotation of the en ligands (~5°) with respect to neighboring chains. This is consistent with a previous conclusion[6a] that the primary difference between the two phases is interchain (orthorhombic) vs intrachain (monoclinic) hydrogen bonding. To elucidate these and other structural features, low-temperature structures of PtBr crystals, with and without Cl^- doping, and pure PtCl crystals are under current investigation.

Figure 3 shows the RR spectra of three $PtBr_{1-x}Cl_x$ samples at excitation energies near the intervalence charge-transfer (IVCT) band edge. These spectra clearly show the effect of increasing PtCl concentration on the ν_1 band. At 1.60-eV excitation, the $PtBr_{0.22}Cl_{0.78}$ and $PtBr_{0.89}Cl_{0.11}$ samples show fine structure (168, 174, and 181 cm^{-1}) in the ν_1 band that is not observed in the spectrum of $PtBr_{0.99}Cl_{0.01}$. An additional weaker component at 171 cm^{-1} is shown by curve resolution to be present in the Cl^--doped crystals. Conversely, the only modes observed for $PtBr_{0.99}Cl_{0.01}$ are the fundamental and its overtone (Figure 3). These results unambiguously demonstrate that the normal chain ν_1 band is at 166 cm^{-1}, that this same mode is shifted to slightly higher frequency in Cl^--doped samples, and that the fine structure corresponds to microstructures, defects, or photoexcited states that are stabilized (pinned) by the presence of Cl^- impurities. In addition to the fine structure near the ν_1 band, the Cl^- impurity leads to new Raman modes at ca. 210, 294, 308, and 324 cm^{-1}. The peak at 210 cm^{-1} is attributed to a local mode of the PtBr chains in the vicinity of the Cl^- dopant (an edge state) while the modes at 294 and 324 cm^{-1} have been attributed to local states in PtCl chains (below and refs 14 and 15).

The mode at ca. 308 cm^{-1} is especially intense in the orthorhombic sample and corresponds to the ν_1 Pt–Cl stretch for $Pt(en)_2Cl_2^{2+}$ units in the crystal. The intensity of this band increases dramatically as the excitation energy is tuned toward 2.41 eV. The RR spectra of $PtBr_{1-x}Cl_x$ (x = 0.01, 0.11, 0.95), acquired with 2.41-eV excitation are displayed in Figure 4. The RR spectrum of PtCl deliberately doped with PtBr, x = 0.95, shows complexities similar to those observed in other mixed-halide solids but primarily exhibits the ν_1 mode of the pure PtCl material.[3a]

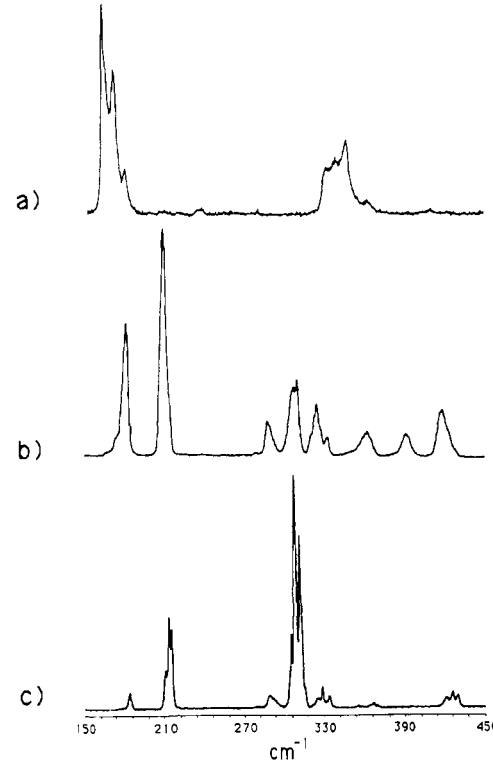

Figure 4. Resonance Raman spectra of (a) $PtBr_{0.99}Cl_{0.01}$, (b) $PtBr_{0.89}Cl_{0.11}$, (c) and $PtBr_{0.05}Cl_{0.95}$ at 2.41-eV excitation.

However, some Raman activity due to $Pt(en)_2Br_2^{2+}$ units is observed at 180 and 210 cm^{-1}. The fine structure that is characteristic of the ν_1 mode for pure PtCl is also observed in the 210-cm^{-1} mode. The origin of this fine structure is not certain; however, the presence of this pattern in the 308 cm^{-1} band observed for the x = 0.95 material may suggest the presence of domains of pure PtCl within the crystal. The defect peaks at 174 and 181 cm^{-1} in $PtBr_{0.99}Cl_{0.01}$ observed with 2.41-eV excitation are, most likely, photoinduced. This is supported by data acquired for this sample at elevated temperatures (150–250 K, not shown), which reveal that these defect modes are nearly absent; if these modes resulted from Cl^- ion doping, they would persist at elevated temperatures. Conversely, the $PtBr_{0.89}Cl_{0.11}$ retains these defect Raman features even at room temperature.[3c] These results demonstrate that the presence of Cl^- in PtBr results in increased stabilization of valence and structural defects.

The RR data suggest that the number of mixed-halide Pt^{IV} sites ($Pt(en)_2ClBr^{2+}$ units) is small despite the relatively high solution concentrations of the mixed halide complexes observed by ^1H NMR. Lattice dynamics calculations[14] indicate that the mode at 324 cm^{-1} (calcd 329 cm^{-1}) could be attributed to the Pt–Cl stretch for the $Pt(en)ClBr^{2+}$ units in the orthorhombic and monoclinic PtBr A samples; the corresponding Pt–Br stretch for this species is calculated to occur at 184 cm^{-1} and may be obscured by the strong defect modes observed at 171–181 cm^{-1}. However, self-consistent phonon calculations performed using a Peierls–Hubbard model indicate that an edge-state mode corresponding to a PtCl segment adjacent to a PtBr segment is expected in the 320-cm^{-1} region.[15] If this latter assignment is correct, there is no evidence for $Pt(en)_2ClBr^{2+}$ units in the mixed-halide sample Raman

(14) Bulou, A.; Donohoe, R. J.; Swanson, B. I. *J. Phys. C*, submitted for publication.
(15) Batistic, I.; Saxena, A.; Bishop, A. R.; Donohoe, R. J.; Swanson, B. I., manuscript in preparation.

spectra. In either event, the Raman intensity for the 324-cm^{-1} feature is weak relative to that of the ν_1 band for $Pt(en)_2Cl_2^{2+}$ units, and we conclude that the concentration of $Pt(en)_2ClBr^{2+}$ units in the mixed samples is small.

In earlier studies of pure PtCl,[3f,g] we observed a RR feature at ca. 287 cm^{-1} that gained intensity upon photolysis within the IVCT band. On the basis of agreement between Peierls–Hubbard model calculations and the observed excitation profile, we attributed this feature to the Pt–Cl stretch for a hole polaron. The 294-cm^{-1} band observed in $PtBr_{1-x}Cl_x$ (x = 0.11 and 0.55) exhibits an excitation profile that is similar to that observed for the hole polaron RR vibration in pure PtCl. Accordingly, we attribute this mode to a hole polaron in the PtCl chains in the mixed-halide solids. At other excitation energies, we observe a peak near 260 cm^{-1} that mimics the excitation profile associated with the electron polaron defect mode in pure PtCl (263 cm^{-1}). More detailed spectral studies of local states and their dependences on Cl^- impurities in PtBr will be reported later.

The results obtained here help clarify the origin of the surprising differences between the RR spectra of PtBr and those of PtI and PtCl: $PtBr_{0.99}Cl_{0.01}$ crystals exhibit RR spectral features that are quite similar to those observed for PtI and PtCl.

Conclusions

These results show that the presence of Cl^- ion impurities in PtBr gives rise to the apparent dispersion and fine structure of the ν_1 mode observed in the RR data upon tuning the excitation energy through the IVCT band and that the PtBr ν_1 mode corresponds to the 166-cm^{-1} component. This is consistent with the previously reported sample dependence[3c] on the relative intensities of the 168–, 171–, 174–, and 181-cm^{-1} component bands, since the amount of PtCl present in PtBr will vary according to the method of preparation and purity of starting materials. Simple thermodynamic considerations demonstrate that the coexistence of $Pt(en)_2Cl_2^{2+}$, $Pt(en)_2Br_2^{2+}$, and $Pt(en)_2BrCl^{2+}$ in both solution and the solids is reasonable and expected using the standard preparative route. The polymorphism exhibited by PtBr at room temperature is suggested to result from variations in the relative concentration of Cl^- impurities and the associated change in T_c for the monoclinic to orthorhombic structural phase transformation. That PtCl can coexist with PtBr in these materials and lead to self-doping is an important consideration for future preparation of either pure or mixed-chain materials.

Acknowledgment. We thank Dr. Ed Garcia for important discussions concerning the crystal structures and structural phase transformations. We also acknowledge professor Susumu Kurita for first pointing out to us that PtCl undergoes a phase change near room temperature. This work was performed under the auspices of the U.S. Department of Energy with support from the Materials Science Division of the O.B.E.S. and the Center for Materials Science at LANL.

Registry No. $[Pt(en)_2Br_2][Pt(en)_2](ClO_4)_4$, 62535-08-4.

Thermal Reactivity of Hydrogenosilsesquioxane Gels

V. Belot, R. Corriu,* D. Leclercq, P. H. Mutin, and A. Vioux

Unité Mixte CNRS/Rhône-Poulenc/USTL, case 007, Université de Montpellier II, Pl. E. Bataillon, F34095 Montpellier Cedex 5, France

Received July 11, 1990

The thermal reactivity under argon, air, and ammonia of the hydrogenosilsesquioxane gels prepared from trichloro- or trialkoxysilane was investigated by using a thermogravimetric analyzer interfaced with a mass spectrometer. Under argon these gels thermally decompose by two different mechanisms: (1) the cleavage of Si–H bonds gives rise to a loss of hydrogen; (2) a redistribution reaction of Si–H and Si–O bonds induces the escape of SiH_4. This second reaction, possibly catalyzed by residual hydroxyl groups, involves the formation of SiH_2 groups as evidenced by IR and solid-state NMR spectroscopies. It accounts for the thermograms obtained under air and ammonia.

Introduction

Previous papers pointed out that hydrogenosilsesquioxane gels $HSiO_{1.5}$ offer particular properties arising from the Si–H bond.[1-4] Thus these gels are hydrophobic unlike silica gels. Moreover they are reactive toward oxygen, chlorine, and alkenes. The thermal nitridation with ammonia provides an efficient route to silicon oxynitride glasses.[3,4]

However $HSiO_{1.5}$ gels decompose thermally under inert atmosphere. Previous authors reported the liberation of hydrogen and postulated thermal dehydrogenation involving the cleavage of the SiH bond.[1,5]

Table I. Conditions of Preparation and Characteristics of $HSiO_{1.5}$ Gels

gel	monomer	monomer concn, mol/L	water concn, mol/L	solvt	% H (theor 1.89)
a	$HSi(OEt)_3$	2.38	7.14	ethanol	1.75
b	$HSiCl_3$	0.66	1.32	THF	1.88
c	$HSiCl_3$	0.88	50	ether	1.88

In this work, pyrolyses under argon, air, or ammonia were monitored by using a thermogravimetric analyzer (TGA/DTA) interfaced with a mass spectrometer. This apparatus allowed the continuous analysis of the gases evolved during thermolysis. The residual solid was studied by IR and solid-state NMR spectroscopies.

(1) Wagner, G. H.; Pines, A. N. *Ind. Eng. Chem.* **1952**, *44*, 321.
(2) Pauthe, M.; Phalippou, J.; Corriu, R.; Leclercq, D.; Vioux, A. *J. Non-Cryst. Solids* **1989**, *113*, 21.
(3) Belot, V.; Corriu, R.; Leclercq, D.; Pauthe, M.; Phalippou, J.; Vioux, A. FR Appl. 88/17,071, Dec 1988.
(4) Pauthe, M.; Phalippou, J.; Belot, V.; Corriu, R.; Leclercq, D.; Vioux, A. *J. Non-Cryst. Solids*, in press.
(5) Wiberg, E.; Simmler, W. *Z. Anorg. Allg. Chem.* **1956**, *283*, 401.

0897-4756/91/2803-0127$02.50/0